ELSEVIER

Journal of Alloys and Compounds 253–254 (1997) 605–608

Journal of ALLOYS AND COMPOUNDS

Electrode characteristics of metal hydride electrodes prepared by mechanical alloying

Chang Bo Jung, Kyung Sub Lee*

Department of Metallurgical Engineering, Hanyang University, Seoul, South Korea 133-791

Abstract

AB(TiFe) and AB_2($ZrCr_2$) type metal hydride have been produced by a mechanical alloying (MA) process and their electrochemical characteristics have been evaluated for use in Ni/MH batteries. Ti–Fe alloys showed an amorphous state after 40 h of ball milling, but Zr–Cr alloys revealed a mixture of nanocrystalline $ZrCr_2$ and an amorphous state. MA Ti–Fe alloys showed a higher discharge capacity and a shorter cyclic life than the arc-melted one; however, MA Zr–Cr alloys had a lower discharge capacity and a longer cyclic life. Substitution of alloying elements such as Ni, Co, Cr, Mo and Ti improved greatly the electrode characteristics.

Keywords: Metal hydride; Mechanical alloying; Electrode characteristics

1. Introduction

Metal hydrides (MH) are currently used for the negative electrode in Ni/MH batteries. A number of alloys are still being investigated; they should have an overall good performance, with characteristics such as high charge capacity, long cyclic life, good dischargeability at low temperature, high current density and low self-discharge [1]. One of the candidate alloys is Ti–Fe; it is an inexpensive and plentiful raw material and has a large hydrogen capacity. However, this system has problems in relation to activation treatment and cycle life [2]. Zr-based Laves phase alloys are also of interest because of their higher discharge capacities, but they have the disadvantage of requiring many charge–discharge cycles for activation [3].

Conventionally MH samples have been prepared by arc melting and remelting several times, and by passing through sieves after mechanical pulverization. However, in this study MH samples were prepared by mechanical alloying (MA) as an alternative method. MA is a high-energy ball milling process that produces alloy powders with precise chemical composition and homogeneous microstructure. More recently, this process has been known to produce powders with unusual characteristics such as nanocrystalline structures, amorphous materials and alloys with extended solubilities [4,5].

2. Experimental details

The starting materials for MA are elemental powders with a particle size of less than 300 mesh (46 μm) and purity 99.9%. The mixed powders were charged and sealed in a cylindrical stainless-steel vial (SUS 304; 110 mm in diameter) together with stainless-steel balls (SUS 304; 4.8 mm diameter). The ball-to-powder weight ratio was 100:1. Before milling, the container was evacuated for 1 h by a mechanical pump (2×10^{-3} torr) and then charged with purified argon. All ball milling was performed using an attritor at a speed of 300 rpm in an argon atmosphere after premilling the powder of the same composition to reduce the possible contamination during the milling process. Table 1 shows the compositions of the alloy produced by MA. Chemical analyses of the ball-milled powders by inductively coupled plasma (ICP) analysis indicate that contamination from the wall of the vial and the balls is negligible. The structures of MA powders were characterized by X-ray diffraction (XRD) analysis using Cu Kα radiation (λ=1.5418 Å).

After milling, the powder was mixed with Ni powder as a current collector at to the ratio 1:1 by adding 5 wt% PTFE (polytetrafluoroethylene) as a binder. The electrodes

*Corresponding author.

0925-8388/97/$17.00
PII S0925-8388(96)03044-7

Table 1
Compositions of alloys produced by MA (mole fraction)

Alloy	Element						
	Ti	Fe	Ni	Co	Mo	Cr	Zr
TF1	1.0	1.0					
TF2	1.0	0.8	0.2				
TF3	1.0	0.5	0.5				
TF4	1.0	0.6	0.1	0.1	0.1	0.1	
ZC1						2.0	1.0
ZC2			1.0			1.0	1.0
ZC3	0.5		1.0			1.0	0.5

were prepared by pressing the powders into a pellet of 10 mm in diameter and about 1 mm in thickness at a pressure of 5 ton cm^{-2}. The electrodes were activated in 6 M KOH at 70 °C for 48 h. The electrochemical tests were performed by the galvanostatic method in 6 M KOH electrolyte. The electrode having the active material of 0.1 g was charged for 25 h and discharged to −0.60 V with respect to S.C.E. at a constant current of 2 mA.

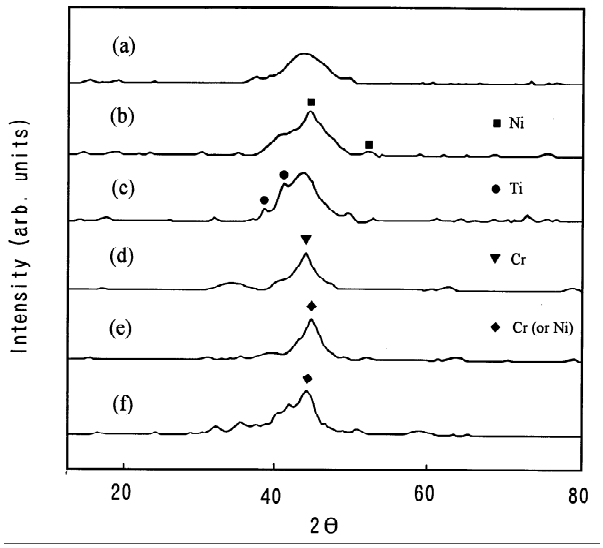

Fig. 1. X-ray diffraction patterns of alloys produced by MA: (a) TF1, (b) TF3, (c) TF4, (d) ZC1, (e) ZC2, and (f) ZC3.

3. Results and discussion

Fig. 1 shows XRD patterns of several alloys after MA. As the milling time increases, the sharp diffraction lines of the elemental powder disappear and the Bragg peaks gradually broaden, indicating amorphous realisation, but no new phase can be detected quantitatively. The Ti–Fe alloy seemed to become amorphous after 40 h ball milling, while the TF3 and TF4 alloys still showed crystalline peaks of Ni and Ti. This means that the latter alloys had a small crystalline portion besides the amorphous phase. Schwarz and Koch [6] have reported a similar observation in the Ni–Ti and Ni–Nb systems. The Zr–Cr system showed a broad diffuse maximum at low diffraction angles and intense Cr (or Ni) peaks at higher angles. It has been suggested that glass formation is due to a solid-state reaction and thus depends on the negative free enthalpy of mixing. Hellstern and Schultz [7] have reported that amorphization by MA is impossible in alloy systems leaving low heats of mixing, such as Cr–Zr and V–Zr alloys. The latter consist of a microscopic mixture of the starting elements after milling. Our XRD results of Zr–Cr were similar to those of Hellstern and Schultz, but the TEM micrographs showed spherical nano-sized $ZrCr_2$ precipitates and an amorphous matrix (Fig. 2). The precipitates were confirmed as C15 (fcc) type in SAD patterns. In an arc-melted ingot cubic C15 and hexagonal C14 phases were observed. The powder size decreased gradually with increased milling time and then reached a constant valve.

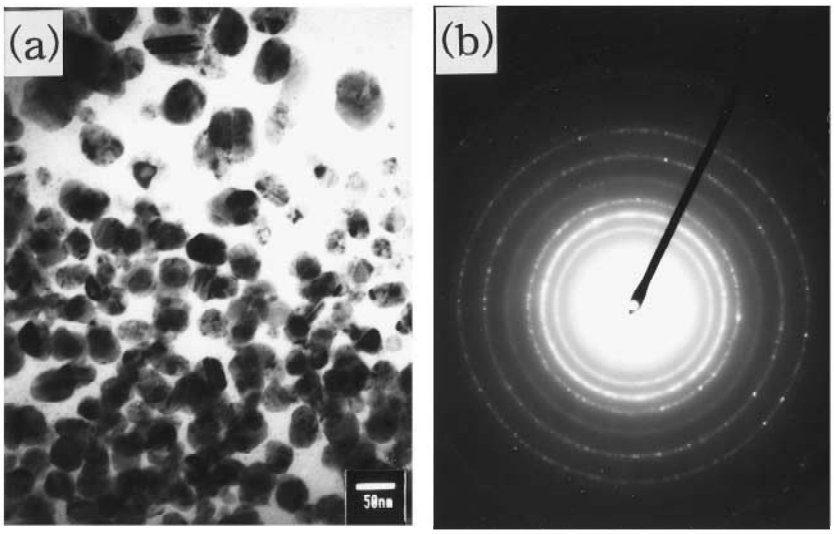

Fig. 2. TEM micrographs of MA ZC1: (a) Bright field image, and (b) SAD pattern.

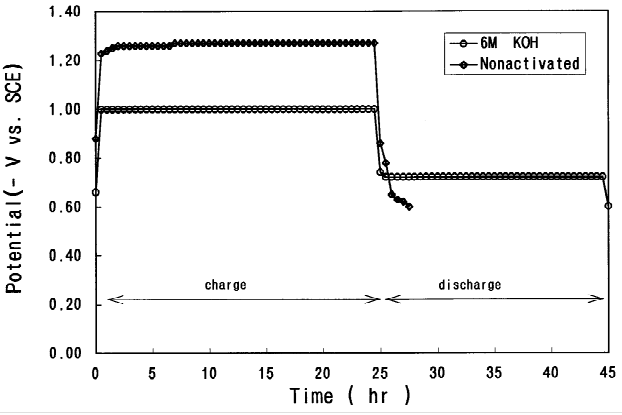

Fig. 3. Cell potentials and capacities of TF4 before and after activation.

The average powder size of TF1 and ZC1 were 18 and 10 μm, respectively. The addition of alloying elements further decreased the powder size to 3 μm in TF4.

Fig. 3 shows the cell potential and discharge capacity of TF4 before and after activation treatment. The charge potential dropped to 1.00 V from 1.27 V by activation treatment. The potential drop could be attributed to the promotion of charge-transfer reaction by the chemically activated surface.

Fig. 4 compares the maximum discharge capacities of mechanically alloyed and arc-melted electrodes. The capacities of MA TF1, TF2 and TF3 were 53, 70 and 190 mA h g^{-1}, respectively, but for the arc-melted ones they were 12, 30 and 65 mA h g^{-1}, respectively. The capacity of MA Ti–Fe electrodes was greater than that of arc-melted ones. This means that the amorphous phase containing a small portion of crystalline phase has a greater capacity than a crystalline when in the Ti–Fe system. Moreover, this figure shows that the discharge capacity increases with the substitution of Ni for Fe. The TF4 electrode showed the greatest discharge capacity (400 mA h g^{-1}) when Fe was replaced by Ni, Cr, Co and Mo. It seems that the additional alloying elements improved the electrochemical performance. The reduced powder size by

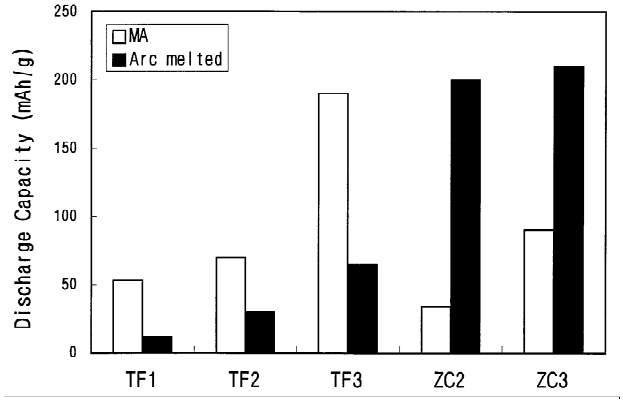

Fig. 4. Maximum discharge capacities of alloys produced by MA or arc melting.

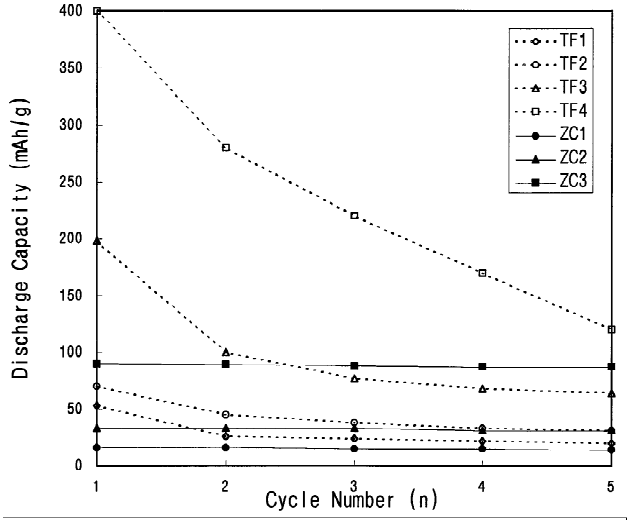

Fig. 5. Discharge capacity–cyclic life characteristics of MA electrodes.

MA may have contributed to the increased discharge capacity. However, the MA Zr–Cr electrode showed a lower discharge capacity than the arc-melted one. The capacity of the arc melted ZC2 and ZC3 were about 200 mA h g^{-1}, and the mechanically alloyed capacities were 34 and 90 mA h g^{-1}, respectively.

Fig. 5 shows the discharge capacities of Ti–Fe and Zr–Cr alloys as a function of cycling. The electrode of the Ti–Fe system displayed a maximum capacity at the first cycle and were degraded within a few cycles. This may be due to the easy formation of the oxide layer during cycling [8]. The discharge capacity of Zr–Cr alloys was not changed much during cycling. Microcracks are usually found in crystalline alloys owing to the repetition of expansion and shrinkage by hydrogen absorption/desorption, but were not observed in the present MA ZrCrNi electrode. Neither plateau pressures nor phase transformations exist in the amorphous state [9]. The discharge capacity of this alloy remained relatively constant because there occurred no microcracking during the test.

4. Conclusions

AB(TiFe) and AB_2($ZrCr_2$) type metal hydride have been produced by MA from elemental powders. Ti–Fe alloys showed an amorphous phase containing a small crystalline portion, but Zr–Cr alloys revealed a mixture of nanocrystalline $ZrCr_2$ and an amorphous phase. Ti–Fe alloys produced by MA had a higher discharge capacity than the arc-melted one and showed a maximum discharge capacity at the first cycle, but were degraded within a few cycles. The discharge capacity of Ti–Fe was greatly improved by substituting alloying elements. The discharge capacities of Zr–Cr alloys produced by MA were lower than that of the arc-melted one, but remained relatively constant during the test.

Acknowledgments

This work was supported by the Ministry of Education Research Fund for Advanced Materials in 1995.

References

[1] T. Sakai, H. Miyamura and I. Uhehara, *J. Alloys Comp., 192* (1993) 158.
[2] M. Boulghallat and N. Gerald, *J. Less-Common Met., 172* (1991) 105.
[3] S.R. Kim and J.Y. Lee, *J. Alloys Comp., 210* (1994) 109.
[4] J.S. Benjamin, *Metall. Trans. A, 1* (1970) 2943.
[5] J.S.C. Jang and C.C. Koch, *J. Mater. Res., 5* (1990) 498.
[6] R.B. Schwarz and C.C. Koch, *Appl. Phys. Lett., 49(3)* (1986) 146.
[7] E. Hellstern and L. Schultz, *Mater. Sci. Eng., 93* (1987) 213.
[8] P. Selvam, B. Viswanathan et al., *J. Less-Common Met., 163* (1990) 89.
[9] J.J.G. Willems, *Philips J. Research, 39* (1984) 1.